


RESEARCH

Open Access



Aorta-specific DNA methylation patterns in cell-free DNA from patients with bicuspid aortic valve-associated aortopathy

Ashna Maredia^{1,2,3}, David Guzzardi³, Mohammad Aleinati^{2,3}, Fatima Iqbal^{2,3}, Arshroop Khaira^{2,3}, Aiswarya Madhu^{2,3}, Xuemei Wang^{2,3}, Alex J. Barker⁴, Patrick M. McCarthy⁵, Paul W. M. Fedak³ and Steven C. Greenway^{1,2,3*} 

Abstract

Background The dilation of the aorta that occurs as a consequence of a congenitally bicuspid aortic valve (BAV) is associated with a risk of dissection, aneurysm or rupture. With progressive aortopathy, surgery is often recommended, but current patient selection strategies have limitations. A blood-based assay to identify those who would most benefit from prophylactic surgery would be an important medical advance. In a proof-of-concept study, we sought to identify aorta-specific differentially methylated regions (DMRs) detectable in plasma cell-free DNA (cfDNA) obtained from patients undergoing surgery for BAV-associated aortopathy.

Methods We used bioinformatics and publicly available human methylomes to identify aorta-specific DMRs. We used data from 4D-flow cardiac magnetic resonance imaging to identify regions of elevated aortic wall shear stress (WSS) in patients with BAV-associated aortopathy undergoing surgery and correlated WSS regions with aortic tissue cell death assessed using TUNEL staining. Cell-free DNA was isolated from patient plasma, and levels of candidate DMRs were correlated with aortic diameter and aortic wall cell death.

Results Aortic wall cell death was not associated with maximal aortic diameter but was significantly associated with elevated WSS. We identified 24 candidate aorta-specific DMRs and selected 4 for further study. A DMR on chromosome 11 was specific for the aorta and correlated significantly with aortic wall cell death. Plasma levels of total and aorta-specific cfDNA did not correlate with aortic diameter.

Conclusions In a cohort of patients undergoing surgery for BAV-associated aortopathy, elevated WSS created by abnormal flow hemodynamics was associated with increased aortic wall cell death which supports the use of aorta-specific cfDNA as a potential tool to identify aortopathy and stratify patient risk.

Keywords DNA methylation, Cell-free DNA, Bicuspid aortic valve, Wall shear stress, Apoptosis

*Correspondence:

Steven C. Greenway
scgreenw@ucalgary.ca

Full list of author information is available at the end of the article



© The Author(s) 2021. **Open Access** This article is licensed under a Creative Commons Attribution 4.0 International License, which permits use, sharing, adaptation, distribution and reproduction in any medium or format, as long as you give appropriate credit to the original author(s) and the source, provide a link to the Creative Commons licence, and indicate if changes were made. The images or other third party material in this article are included in the article's Creative Commons licence, unless indicated otherwise in a credit line to the material. If material is not included in the article's Creative Commons licence and your intended use is not permitted by statutory regulation or exceeds the permitted use, you will need to obtain permission directly from the copyright holder. To view a copy of this licence, visit <http://creativecommons.org/licenses/by/4.0/>. The Creative Commons Public Domain Dedication waiver (<http://creativecommons.org/publicdomain/zero/1.0/>) applies to the data made available in this article, unless otherwise stated in a credit line to the data.

Background

The aortopathy that occurs as a consequence of a congenitally bicuspid aortic valve (BAV) is associated with a risk of dissection, aneurysm or rupture (1). The etiology of BAV-associated aortopathy appears to be multifactorial and related to inherent genetic defects (2) combined with hemodynamic wall shear stress (WSS) created by turbulence across the abnormal valve (3–6). Increased aortic WSS leads to the degradation of elastin and the dysregulation of extracellular matrix proteins which are linked to smooth muscle cell death (7–9). With progressive aortopathy, aortic valve replacement surgery is often recommended, but patient selection is controversial and often dependent upon individual and institutional practice (10–14). A blood-based assay, potentially in combination with advanced imaging techniques, to identify those who would most benefit from prophylactic surgery would be a significant advance (15).

Cell-free DNA (cfDNA) refers to fragments of genomic DNA released into the blood during cellular apoptosis (16–18). The accessibility of plasma cfDNA and its retention of genetic and epigenetic changes have resulted in the development of cfDNA-based diagnostic assays for diverse human diseases and applications (19–21). DNA methylation is an important regulator of gene expression and determinant of cell specialization (22), and tissue-specific differentially methylated regions (DMRs) have been identified for multiple human cells, tissues and organs (20). We hypothesize that aorta-specific DMRs detectable in cfDNA will allow the noninvasive assessment of disease and the prediction of important clinical events and enable precision medicine for optimal

management of patients with aortopathy and highly variable individual risk.

In this pilot study, we identified novel and unique aorta-specific DMRs that could be measured in human plasma cfDNA obtained from patients with BAV-associated aortopathy who were undergoing surgery. We identified the relationship between elevated WSS and cell death in the ascending aorta of human BAV patients to demonstrate the biological rationale for cfDNA as a biomarker of aortopathy and identified an association between aorta-specific cfDNA levels, WSS and aortic wall cell death.

Results

Cell death is increased in aortic regions of elevated wall shear stress

For all individual BAV patients, cell death, as assessed using terminal deoxynucleotidyl transferase dUTP nick end labeling (TUNEL) and 4',6-diamidino-2-phenylindole (DAPI) staining, was increased in regions of the ascending aorta that demonstrated elevated WSS compared to the regions of normal WSS as determined by cardiac magnetic resonance imaging (CMR) and this difference was significant for the paired comparisons and pooled data (Fig. 1). The mean cell death (mean percent colocalization of TUNEL and DAPI staining) in the regions with normal WSS was $7.98 \pm 5.94\%$ compared to $13.74 \pm 5.49\%$ in regions with elevated aortic WSS ($p=0.0027$). This data demonstrates that regions of abnormal hemodynamics are associated with increased levels of aortic tissue cell death. However, we did not observe a consistent relationship between maximal aortic diameter and WSS or cell death. There was no significant relationship found between levels of aorta-specific

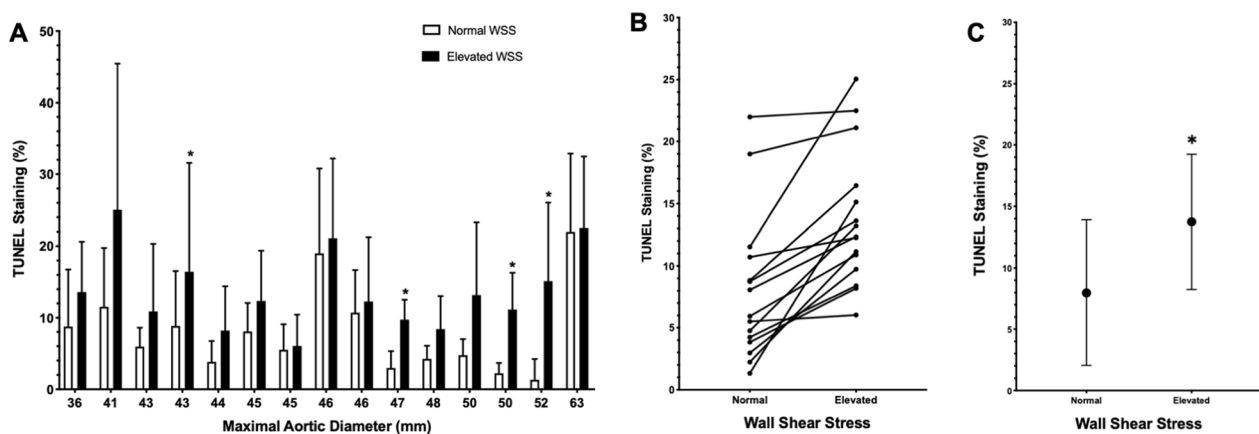


Fig. 1 **a** Aortic wall cell death (indicated by percentage of TUNEL-positive cells) for 15 patients with varying maximal aortic diameters comparing regions of normal and elevated aortic WSS. Data presented are mean \pm SD with * indicating $p < 0.05$ as determined by a Mann–Whitney U test. **b** Paired patient data were found to be significantly different ($p = 0.00006$) using the Wilcoxon signed rank test. **c** Summarized data. Data are mean \pm SD with significantly greater cell death in regions of elevated WSS as determined by a Mann–Whitney U test ($p = 0.0027$)

cfDNA and cell death in regions with normal WSS (Additional file 1: Fig. S3), and total cfDNA did not correlate with levels of cell death in regions of increased WSS (Additional file 1: Fig. S4).

Identification of aorta-specific differentially methylated regions

After comparing the aortic methylome to methylomes from 19 tissues, we identified 446 putative aortic-specific DMRs with a minimum mean methylation difference of 60%. Comparing the aorta methylome to 14 methylomes from various hematopoietic cells identified 181 aorta-specific DMRs with a minimum mean methylation difference of 90% (Fig. 2). There were 24 DMRs on autosomal chromosomes that were common to both datasets and after further testing, we selected four DMRs for further study, all of which were hypomethylated in the aorta (Table 2). The DMR on Chr 11 (position Chr 11:3,168,734–3,168,832) is 73 bp in length, contains 6 CpG sites and is predicted in silico to have the lowest specificity for the aorta in comparison with other tissues but the highest specificity in comparison with hematopoietic cells. The DMR on Chr 18 (position Chr 18:74,171,459–74,171,505) contains 8 CpG sites over

46 bp. The DMR on Chr 20 (position Chr 20:45,860,400–45,860,466) contains 6 CpG sites over 65 bp with the greatest predicted specificity for the aorta in comparison with other tissues. The DMR on Chr 22 (position Chr 22:27,999,645–27,999,717) contains 7 CpG sites over 72 bp. Given the unbiased nature of our enquiry, we were not surprised to see that the regions identified were not specific to genes known to be associated with cardiovascular disease or development. The Chr 11 DMR is found within the *OSBPL5* (oxysterol binding protein-like 5) gene which is an intracellular lipid receptor. The Chr 18 DMR is found within the *ZNF516* (zinc finger protein 516) gene, the Chr 20 DMR is within the *ZMYND8* (zinc finger, MYND-type containing 8) gene, and the Chr 22 DMR is not associated with a coding region. A review of these four regions using the ENCODE database did not identify obvious regulatory functions.

In vitro testing of aorta-specific DMRs

To further test the tissue specificity of the DMRs that we had identified, we obtained gDNA from 14 different human tissues and organs encompassing all three developmental germ layers and compared the measured methylation status in each tissue to the aorta for each

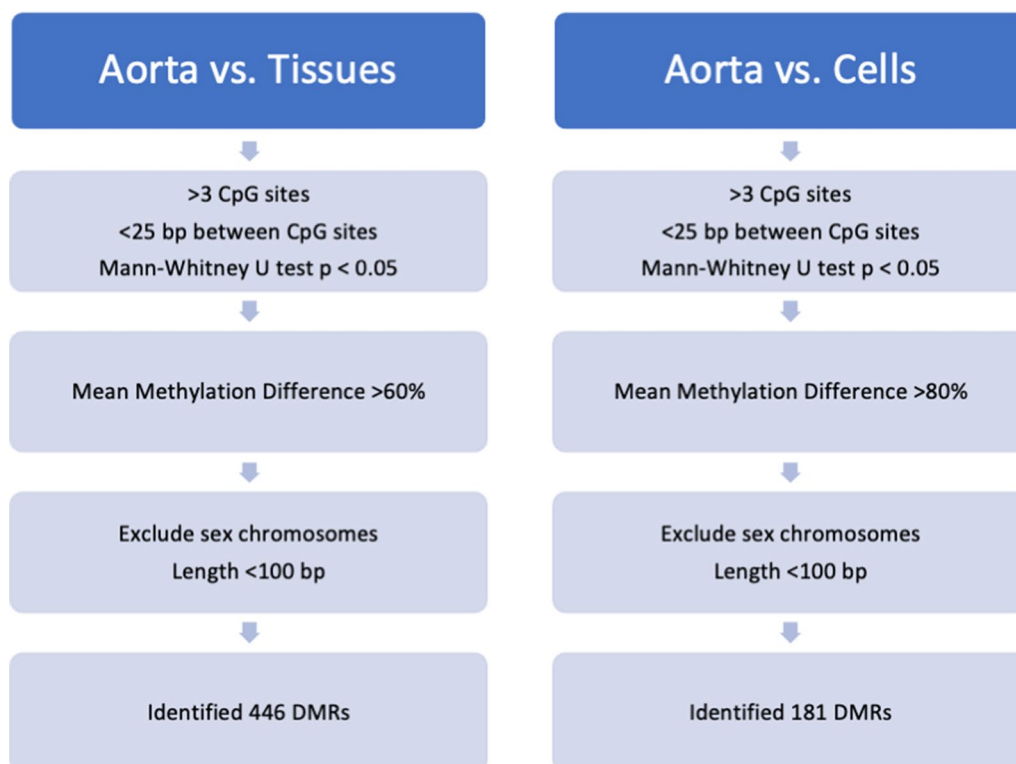


Fig. 2 Bioinformatics pipeline used to identify DMRs. Two separate comparisons were conducted in parallel, comparing a human aorta methylome to methylomes from 21 tissues and 14 types of hematopoietic cells to identify 446 and 181 DMRs, respectively. A total of 24 candidate aorta-specific DMRs were shared by both datasets

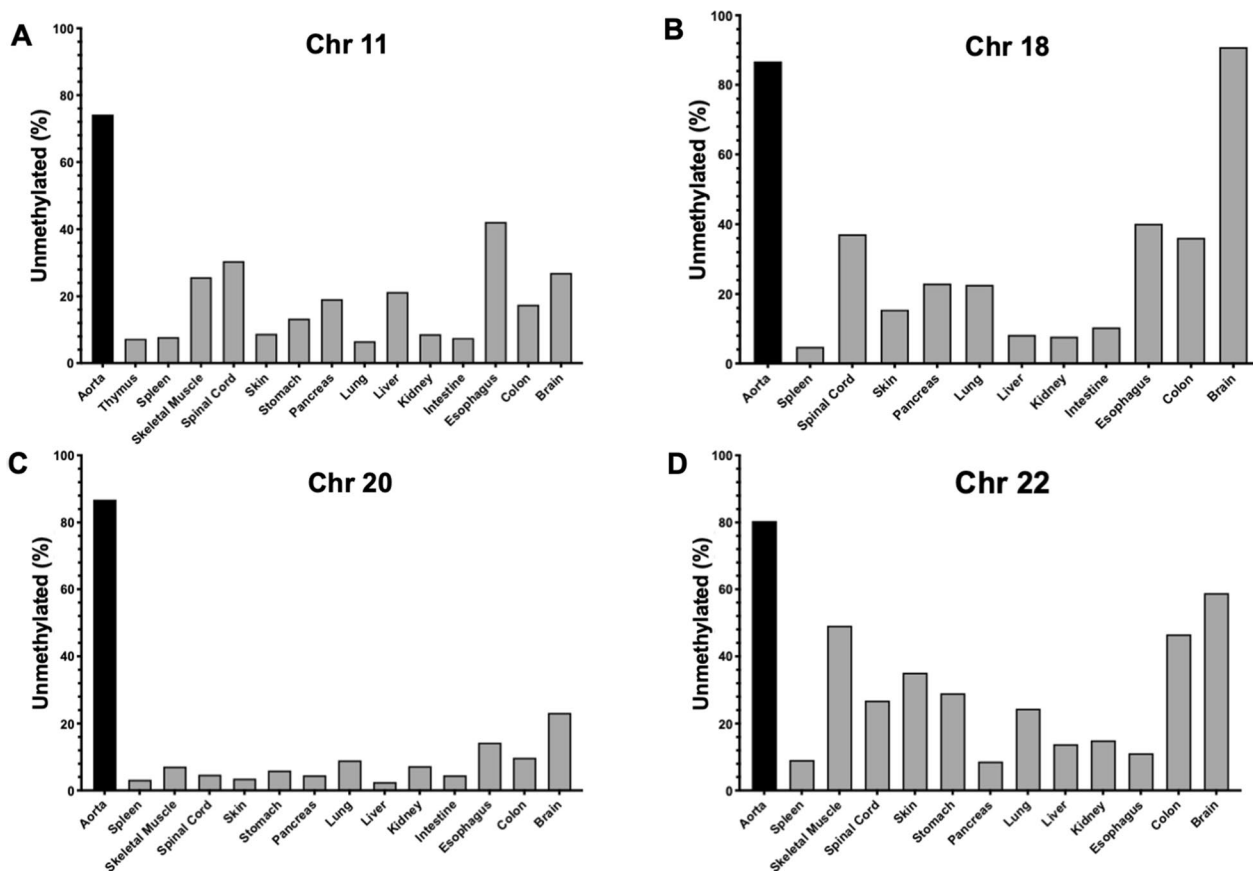


Fig. 3 **a** Percentage of unmethylated CpG sites for the Chr 11 DMR in aorta and other human tissues and organs. **b** Percentage of unmethylated CpG sites for the Chr 18 DMR in aorta and other human tissues and organs. **c** Percentage of unmethylated CpG sites for the Chr 20 DMR in aorta and other human tissues and organs. **d** Percentage of unmethylated CpG sites for the Chr 22 DMR in aorta and other human tissues and organs

DMR. For the Chr 11 DMR, 74.2% of the reads from the aorta were unmethylated, for the Chr 18 DMR, 86.8% of the reads were unmethylated, 86.8% of the reads were unmethylated for the Chr 20 DMR, and for the Chr 22 DMR, 80.4% of the aorta reads were unmethylated (Fig. 3). The Chr 11 and Chr 20 DMRs were mostly methylated across all tissues, but the Chr 18 DMR was mostly unmethylated in the brain with levels similar to that seen in the aorta and also showed low levels of methylation in the spinal cord, esophagus and colon. For the Chr 22 DMR, it was highly unmethylated in skeletal muscle, colon and brain.

Correlation of aorta-specific cfDNA levels with clinical severity of aortopathy

Using cfDNA isolated from patient plasma, the aorta-specific cfDNA levels for 23 BAV patients were determined using the DMRs located on Chr 11, 18, 20 and 22 (Fig. 4). In this cohort of patients with severe disease, none of the aorta-specific DMRs showed an association

with aortic diameter as measured using CMR. Similarly, total plasma cfDNA also did not correlate with aortic size (Additional file 1: Fig. S1). However, levels of aorta-specific cfDNA as determined based on our 4 DMRs did show a positive correlation with levels of cell death in the regions of elevated aortic WSS (Fig. 5). This correlation was statistically significant for the Chr 11 DMR ($R^2=0.59$, $p=0.0035$), the Chr 18 DMR ($R^2=0.62$, $p=0.012$) and the Chr 22 DMR ($R^2=0.52$, $p=0.0078$). The Chr 20 DMR did not show a significant correlation ($R^2=0.55$, $p=0.06$). However, our candidate DMRs showed no significant correlation with several histological markers associated with elastin degradation (Additional file 1: Table S4) and dysregulation of ECM proteins (concentrations of MMP types 1, 2 and 3, TGF β -1 and TIMP-1, Additional file 1: Table S5) known to occur in aortopathy. Due to low plasma volumes resulting in low yields of cfDNA, some patient cfDNA samples could not be sequenced which affected the number of data points for each DMR as displayed in Figs. 4 and 5.

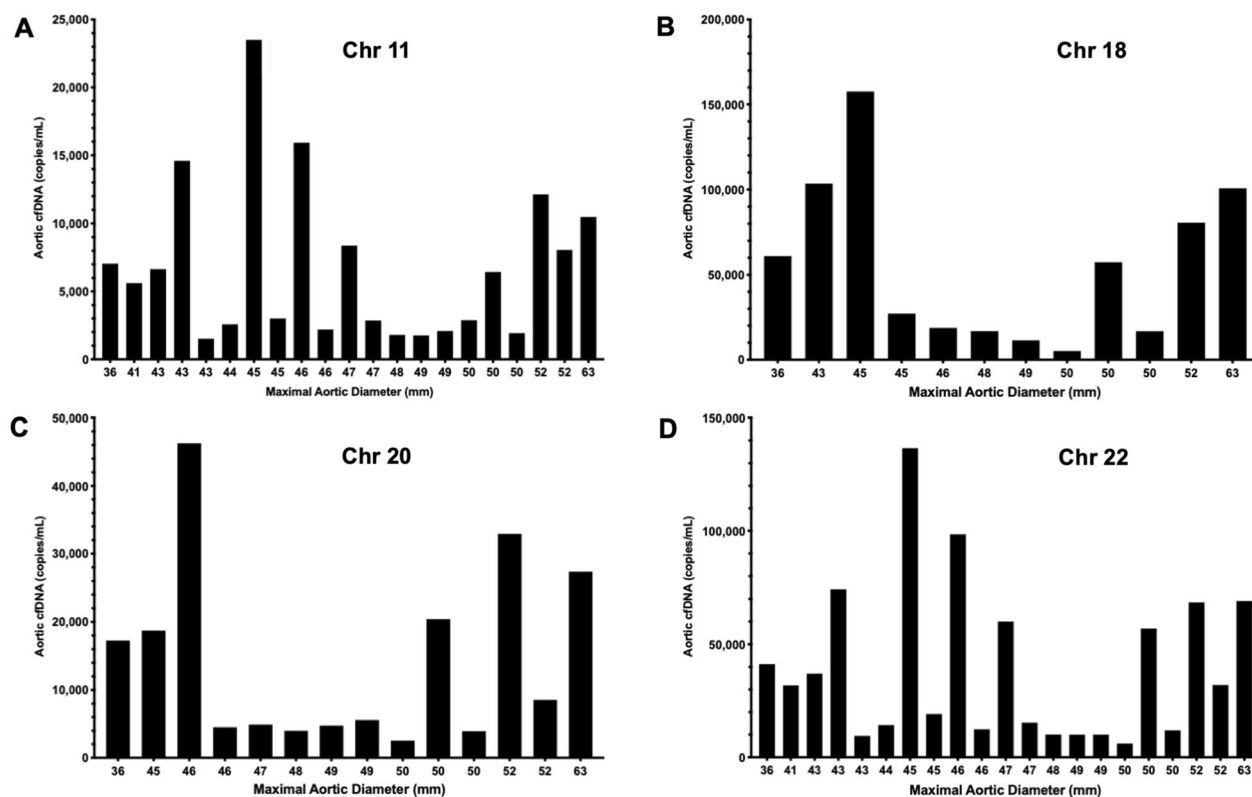


Fig. 4 **a** Aorta-specific cfDNA concentration as determined by the Chr 11 DMR for 23 patients sorted by maximal aortic diameter. **b** Aorta-specific cfDNA concentration as determined by the Chr 18 DMR for 23 patients sorted by maximal aortic diameter. **c** Aorta-specific cfDNA concentration as determined by the Chr 20 DMR for 23 patients sorted by maximal aortic diameter. **d** Aorta-specific cfDNA concentration as determined by the Chr 22 DMR for 23 patients sorted by maximal aortic diameter

Discussion

Using publicly available human methylomes, we bioinformatically identified 24 candidate aorta-specific DMRs. A subset was chosen for further evaluation, and the Chr 11 DMR demonstrated specificity for the aorta and significant correlation with aortic wall apoptosis. Our results in this proof-of-concept study demonstrate the feasibility of identifying a peripheral blood marker for aortopathy based on DNA methylation patterns and the importance of *in vitro* validation studies.

In this study, the levels of cell death were measured using the TUNEL assay and colocalized to individual cells using nuclear DAPI staining in aortic tissue samples from regions of elevated and normal WSS in BAV patients requiring surgery. We found that cell death was not associated with maximal aortic diameter but was associated with increased WSS. Our data suggest an association between abnormal hemodynamics and ongoing tissue injury that is independent of aortic size. As these BAV patients experience chronic localized elevated WSS, we hypothesize that the greater levels of cell death in these regions would lead to the depletion of vascular

smooth muscle cells and likely negatively impact the integrity of the aorta. Our subsequent data suggest that this increased cell death due to hemodynamic stress is detectable by circulating aorta-specific cfDNA identified through unique DNA methylation patterns. Further work is necessary to assess levels of aorta-specific cfDNA in the plasma from patients with milder forms of BAV-associated aortopathy.

DNA methylation plays a critical role in regulating gene expression and thus cellular differentiation. Tissue-specific methylation patterns are conserved within a tissue type and to a large degree across individuals (23). This consistency is critical for the potential development of a universal, minimally invasive cfDNA-based assay. From the 24 putative aorta-specific DMRs identified, 4 were selected for detailed study based in part on their computationally predicted specificity for the aorta. The specificity of the 4 DMRs on Chr 11, 18, 20 and 22 was then tested *in vitro* using a panel of DNA isolated from multiple human tissues. We found that the methylation differences between the aorta and several tissues and organs were smaller than the *in silico* predictions for

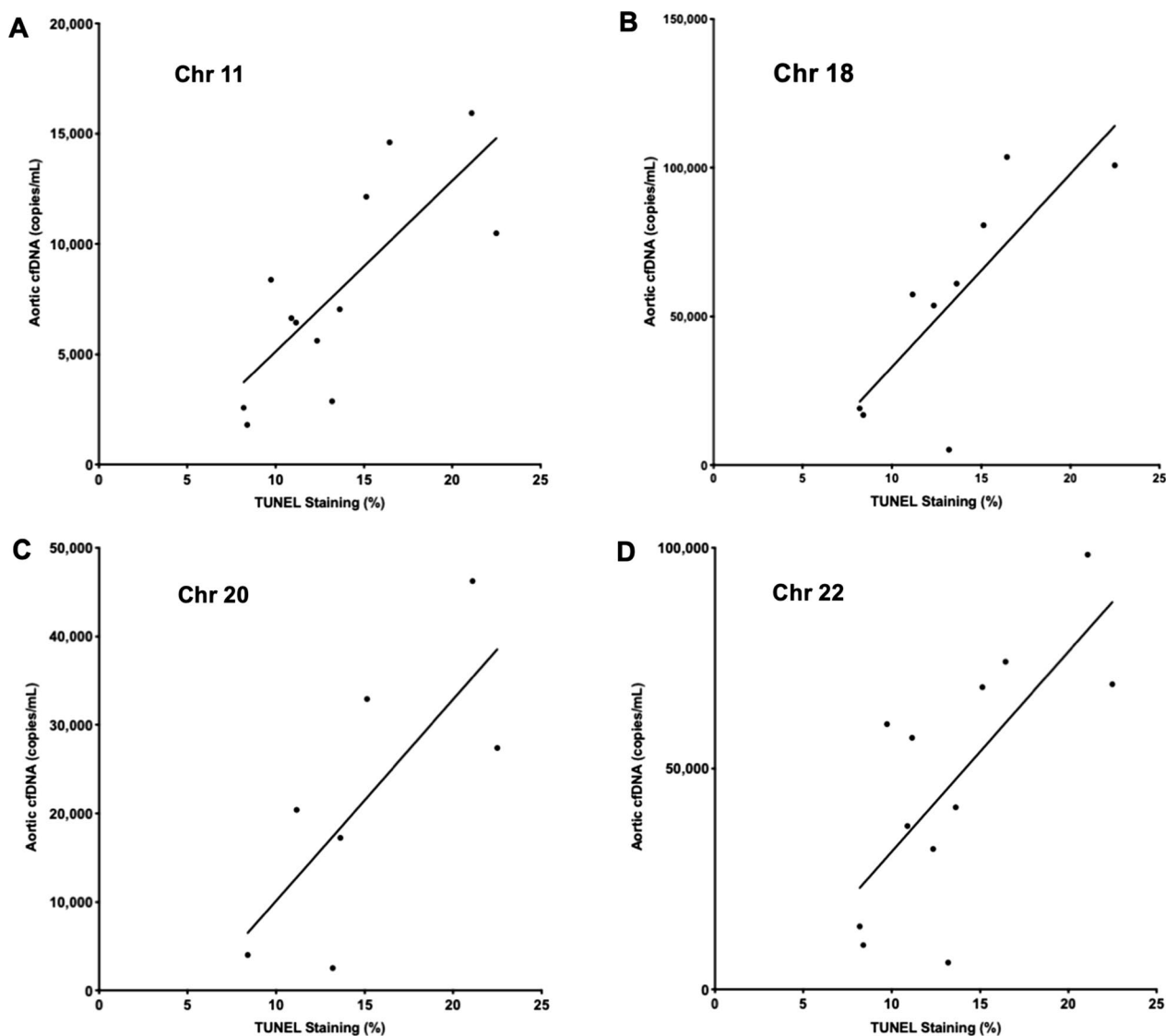


Fig. 5 **a** Significant correlation (R^2 0.59, $p=0.0035$) between levels of aorta-specific cfDNA as measured using the Chr 11 DMR and TUNEL staining in regions of elevated WSS. **b** Significant correlation (R^2 0.62, $p=0.012$) between levels of aorta-specific cfDNA as measured using the Chr 18 DMR and TUNEL staining in regions of elevated WSS. **c** Non-significant correlation (R^2 0.55, $p=0.06$) between levels of aorta-specific cfDNA as measured using the Chr 20 DMR and TUNEL staining in regions of elevated WSS. **d** Significant correlation (R^2 0.52, $p=0.0078$) between levels of aorta-specific cfDNA as measured using the Chr 22 DMR and TUNEL staining in regions of elevated WSS

many of the DMRs. Importantly, the DMR on Chr 18 was found to be equally hypomethylated in the brain and the aorta and therefore can be eliminated as an aorta-specific biomarker.

Our candidate DMRs were also evaluated using plasma cfDNA obtained from patients with BAV-associated aortopathy undergoing surgery. The levels of both aorta-specific and total plasma cfDNA did not correlate with maximal aortic diameter which is consistent with numerous studies documenting that aortic dimensions (both absolute diameter and rate of progression) are insufficient for assessing the severity

of aortopathy and in estimating the underlying risk for aortic rupture (12, 24–26). However, although our aorta-specific DMRs did not correlate with aortic dimension, three of them did correlate significantly with levels of cell death in the aorta. This encouraging result provides a rationale for cfDNA as a biomarker for aortic cell death which, as we have also shown, is associated with elevated regions of WSS. Although our candidate DMRs showed no significant correlation with several histological markers associated with elastin degradation and dysregulation of ECM proteins known to occur in aortopathy, the integrity of

the aortic wall is impacted by many factors, including apoptosis that leads to the depletion of vascular smooth muscle cells (27–29). Regardless of the mechanism of cell death, DNA fragmentation and its release into the circulation are a common endpoint. Thus, the level of aorta-specific cfDNA is potentially an independent and end-stage measure of aortic cell death, regardless of mechanism.

One of the several limitations of our study was the availability of only a single methylome for the aorta in the data format that we required. Furthermore, the precise origin of this tissue was unknown. In the future, generating multiple methylomes from the aortic root and ascending aorta may improve the specificity and utility of biomarkers that are developed for BAV-associated aortopathy. Additional limitations were the relatively small, retrospective sample population and the absence of plasma cfDNA from individuals with BAV not undergoing surgery.

Conclusions

In conclusion, elevated WSS created by abnormal flow hemodynamics is associated with increased aortic wall cell death. This finding supports the use of cfDNA as a potential tool to identify aortopathy and stratify patient risk. By leveraging publicly available data and developing a novel bioinformatics pipeline, we identified candidate aorta-specific DMRs that were detectable in cfDNA. Subsequent *in vitro* studies suggest that the Chr 11 DMR is specific for the aorta, and we have shown that it also correlated with the severity of aortic wall apoptosis in patients with severe aortopathy requiring surgery. However, this intriguing finding needs to be replicated and validated in a prospective study and explored in patients with milder forms of aortopathy.

Methods

Patient data

This study was approved by the Research Ethics Boards at the University of Calgary and Northwestern University. After obtaining informed written consent, blood and matched tissue samples from adult patients with BAV undergoing aortic surgery were obtained (Table 1). All patients ($n=23$) and healthy age-matched controls with tricuspid aortic valves and no documented cardiovascular disease ($n=10$) underwent 4D-flow CMR to visualize aortic blood flow patterns, generate WSS heat maps and calculate WSS values as previously described (9). Data from the healthy controls (who did not undergo surgery) were used to construct a physiologically normal heat map of aortic flow, and regions of depressed, normal and elevated WSS were determined for each BAV patient relative to this control map. Aortic wall tissue samples

Table 1 Patient clinical characteristics

Parameter	Study population
Age (years)	49.3 ± 14.9
Male (%)	20 (87)
BAV classification	
Type 0 (lateral)	1
Type 1 (RL)	15
Type 2 (RN)	7
Maximum aortic diameter (cm)	4.67 ± 0.52
Aortic valve surgical procedure	
Repair	3
Replacement	20
Ascending aorta surgical procedure	
Ascending aorta replacement	20
Root replacement	2
Hemi-arch reconstruction	1

Data reported as *n* or mean with standard deviation. BAV types were grouped according to the Sievers classification scheme (36). *RL*, right-left coronary cusp fusion; *RN*, right-non-coronary cusp fusion

collected during surgery were flash frozen and then paraffin-embedded.

Isolation of cfDNA

Adult BAV patients were recruited, and 8–10 mL of blood was collected before the CMR imaging required for their surgery. The blood was centrifuged at 1900×*g* for 10 min, and then, the isolated plasma was centrifuged at 4 °C at 13,000 RPM for 15 min. The resulting plasma was stored at – 80 °C until use. Patient cfDNA was isolated from 2 mL of plasma using the semi-automated MagNA Pure 24 System (Roche) according to the manufacturer's instructions. The cfDNA yield was quantified by TapeStation (Agilent) and stored at – 80 °C.

TUNEL assay for cell death

Regions of the ascending aorta with the highest and lowest WSS scores (one of each) were stained for quantification of cell death. Paraffin tissue sections mounted on glass slides were used for terminal deoxynucleotidyl transferase dUTP nick end labeling (TUNEL, Promega) and 4',6-diamidino-2-phenylindole (DAPI, ThermoFisher Scientific) staining according to the manufacturer's instructions. Stained tissue slides were imaged (10–20 images per sample to capture the entire tissue section) using a spinning disk confocal super resolution microscope (SpinSR10, Olympus) at 10X magnification and then analyzed using the ImageJ plugin Fiji (30). Green (488 nm) TUNEL staining was colocalized to blue (405 nm) DAPI staining (Additional file 1: Fig. S2), and the percent colocalization/cell death was determined for

each image. Detailed experimental details are described in Supplementary Material.

Identification of aorta-specific DMRs

Publicly available methylomes from human hematopoietic cells ($n=14$), non-aortic tissues ($n=21$) and aorta ($n=1$) were obtained from the Roadmap and Blueprint Epigenomic projects (Additional file 1: Table S1) (31, 32). The software package Metilene identified DNA regions that were significantly differentially methylated (mean difference >10%) based on a Mann–Whitney U test ($\alpha=0.05$) (33). Other parameters included a minimum of 4 CpG sites per DMR, <25 base pairs (bp) separating each of the CpG sites and a total DMR length of <100 bp to enable detection in fragments of cfDNA which are ~140–160 bp in length. A second filtering step identified aortic DMRs with a mean methylation difference >60% for non-aortic tissues and >80% for hematopoietic cells. Comparisons were made separately to enable stringent exclusion of DMRs in peripheral lymphocytes which produce the majority of cfDNA in the circulation. The filtering cutoffs chosen resulted in a sufficient number of DMRs within each interrogated group to enable the identification of DMRs that were common to both groups. Shared DMRs on autosomal chromosomes (sex chromosomes were excluded to avoid dosage effects) identified from the comparison of aorta and non-aorta tissue methylomes ($n=446$) and from aortic tissue compared to hematopoietic cell methylomes ($n=181$) provided a total of 24 candidate aorta-specific DMRs (Fig. 2 and Additional file 1: Table S2). Specific details of the bioinformatics used are described in Supplementary Material.

For 10 candidate DMRs with the highest aorta specificity, sequences containing the DMR of interest and 100 bp upstream and downstream were taken from a methylome of the aorta (GSM983648) generated by the NIH Roadmap Epigenomics project. These sequences were used as input for MethPrimer (34) to generate primers for amplification of the DMRs from bisulfite-converted genomic DNA (gDNA). Primers did not contain CpG islands and contained at least two non-CpG cytosines. Total product size was constrained to <150 bp to enable amplification from cfDNA. Optimal annealing temperatures were determined for all DMRs. From these, four DMRs on chromosomes (Chr) 11, 18, 20 and 22 were chosen for further study as these regions amplified readily with no off-target products (Table 2). Sequences and optimal annealing temperatures for the primers used to amplify the DMRs are presented in Additional file 1: Table S3.

To confirm the specificity of our DMRs identified in silico, we used a commercial panel (Zyagen) of gDNA from human brain, colon, esophagus, small intestine, kidney,

Table 2 Four candidate aorta-specific DMRs

DMR				Mean methylation difference (%)	
	Chr	Start position	Length	CpG	Non-aortic tissues
11	3,168,734	73	6	70.60	92.75
18	74,171,459	46	8	74.26	91.27
20	45,860,400	65	6	86.88	81.01
22	27,999,645	72	7	75.36	91.28

Data presented for the four DMRs studied include chromosomal location, length (in base pairs), number of CpG sites and methylation differences between the aorta and pooled non-aortic tissues and hematopoietic cells as determined computationally. All DMRs presented are hypomethylated in the aorta compared to non-aortic tissues and hematopoietic cells.

Chr, chromosome; *CpG*, cytosine–guanine nucleotides

liver, lung, pancreas, stomach, skin, spinal cord, skeletal muscle, spleen and thymus to compare methylation levels for all 4 DMRs across tissues in comparison with aorta tissue. Patient cfDNA and panel gDNA were bisulfite converted using the Epiect Bisulfite Kit (Qiagen) with elution performed twice using 20 L of buffer EB warmed to 56 °C to improve yields. Bisulfite-converted DNA was used for PCR amplification of the DMRs, and products were visualized on a 3% Tris-Acetate-EDTA agarose gel and quantified by TapeStation (Agilent).

Next-generation sequencing

For quantification of methylation, PCR amplicons were pooled in equimolar concentrations for sequencing on an Illumina MiSeq. Libraries were sequenced using the MiSeq reagent kit v3 (150 cycles) to produce 2×75 bp paired-end reads. The quality of each sequenced pool was assessed using FastQC (35). The bisulfite sequencing plugin for the CLC Genomics Workbench (Qiagen) was utilized to analyze the reads which were mapped to the hg19 reference genome with a minimum acceptable alignment of >80%. Methylation levels were determined for each individual CpG site within each DMR, and mean methylation levels were calculated.

Determination of cfDNA concentrations

The concentration of cfDNA (ng/mL) extracted from 2 mL of patient plasma was divided by 0.00303 ng (mass of a single human genome) to determine the total concentration of cfDNA (copies/mL) in recipient plasma (20). To determine the absolute concentration of each DMR, the copies/mL was multiplied by the fraction of unmethylated molecules within the given pool of amplicons as determined from the analysis of the bisulfite-sequenced reads.

Statistics

Statistical analysis was performed using GraphPad Prism 8.0. The percentage of cell death in the aortic tissue is presented as a mean \pm standard deviation. The Shapiro–Wilk test was used to determine normality. For cell death, a paired comparison between regions of normal and elevated WSS was conducted for each patient using a Wilcoxon signed rank test and the comparison between pooled patients was performed using the Mann–Whitney test with $p < 0.05$ considered to be significant. Linear regression to calculate R^2 was used to correlate the DMR-specific cfDNA levels with the percentage of aortic wall cell death as reported in Additional file 1: Table S5.

Abbreviations

BAV	Bicuspid aortic valve
cfDNA	Cell-free DNA
Chr	Chromosome
CMR	Cardiac magnetic resonance imaging
CpG	Cytosine–guanine nucleotides
DAPI	4',6-Diamidino-2-phenylindole
DMR	Differentially methylated region
gDNA	Genomic DNA
MRI	Magnetic resonance imaging
PCR	Polymerase chain reaction
TUNEL	Terminal deoxynucleotidyl transferase dUTP nick end labeling
WSS	Wall shear stress

Supplementary Information

The online version contains supplementary material available at <https://doi.org/10.1186/s13148-021-01137-y>.

Additional file 1. Supplementary Material.

Acknowledgements

We would like to thank the nurses and staff involved in the collection of all patient samples and Leo Dimnik for his assistance in the automated isolation of cfDNA. We acknowledge the imaging support provided by the core imaging facility in the Hotchkiss Brain Institute and the sequencing expertise provided by the Centre for Health Genomics and Informatics at the University of Calgary.

Authors' contributions

AM, DG, MA, FI, AK, AM and XW performed all experiments and analysis. AJB and PWMF supplied clinical and imaging data. PMM supplied patient tissue, plasma and clinical information. PWMF and SCG provided project conceptualization, funding and supervision. AM and SCG wrote the manuscript with input from all authors. All authors read and approved the final manuscript.

Funding

Funding was provided by the University of Calgary and Northwestern University and grant R01HL133504 from the NIH. SCG is supported by the Alberta Children's Hospital Foundation.

Availability of data and materials

Data can be shared upon written request to the corresponding author.

Declarations

Ethics approval and consent to participate

This study was approved by the Research Ethics Boards at the University of Calgary and Northwestern University.

Competing interests

The authors declare no competing interests.

Author details

¹Department of Biochemistry and Molecular Biology, Cumming School of Medicine, University of Calgary, Calgary, AB, Canada. ²Department of Pediatrics and Alberta Children's Hospital Research Institute, Cumming School of Medicine, University of Calgary, Calgary, AB, Canada. ³Department of Cardiac Sciences and Libin Cardiovascular Institute, Cumming School of Medicine, University of Calgary, Calgary, AB, Canada. ⁴Department of Radiology and Bio-engineering, University of Colorado Anschutz Medical Campus and Children's Hospital Colorado, Aurora, CO, USA. ⁵Division of Cardiac Surgery, Northwestern Medicine, Chicago, IL, USA.

Received: 5 April 2021 Accepted: 19 July 2021

Published: 28 July 2021

References

- Verma S, Siu SC. Aortic dilatation in patients with bicuspid aortic valve. *N Engl J Med*. 2014;370:1920–9.
- Sillesen A-S, et al. Prevalence of bicuspid aortic valve and associated aortopathy in newborns in Copenhagen, Denmark. *JAMA*. 2021;325:561–7.
- Huntington K, Hunter AG, Chan KL. A prospective study to assess the frequency of familial clustering of congenital bicuspid aortic valve. *J Am Coll Cardiol*. 1997;30:1809–12.
- Gago-Diaz M et al. The genetic component of bicuspid aortic valve and aortic dilation. An exome-wide association study. *J Mol Cell Cardiol*. 2017;102:3–9.
- Barker AJ, et al. Bicuspid aortic valve is associated with altered wall shear stress in the ascending aorta. *Circ Cardiovasc Imaging*. 2012;5:457–66.
- Barker AJ, Markl M, Fedak PWM. Assessing wall stresses in bicuspid aortic valve-associated aortopathy: forecasting the perfect storm? *J Thorac Cardiovasc Surg*. 2018;156:471–2.
- Fedak PW, et al. Clinical and pathophysiological implications of a bicuspid aortic valve. *Circulation*. 2002;106:900–4.
- Fedak PW, et al. Vascular matrix remodeling in patients with bicuspid aortic valve malformations: implications for aortic dilatation. *J Thorac Cardiovasc Surg*. 2003;126:797–806.
- Guzzardi DG, et al. Valve-related hemodynamics mediate human bicuspid aortopathy: insights from wall shear stress mapping. *J Am Coll Cardiol*. 2015;66:892–900.
- Borger MA, et al. The American Association for thoracic surgery consensus guidelines on bicuspid aortic valve-related aortopathy: full online-only version. *J Thorac Cardiovasc Surg*. 2018;156:e41–74.
- Erbel R et al. 2014 ESC Guidelines on the diagnosis and treatment of aortic diseases: Document covering acute and chronic aortic diseases of the thoracic and abdominal aorta of the adult. The Task Force for the Diagnosis and Treatment of Aortic Diseases of the European Society of Cardiology (ESC). *Eur Heart J*. 2014;35:2873–2926.
- Wasfy JH, Armstrong K, Milford CE, Sundt TM. Bicuspid aortic disease and decision making under uncertainty—the limitations of clinical guidelines. *Int J Cardiol*. 2015;181:169–71.
- Della Corte A et al. Risk stratification in bicuspid aortic valve aortopathy: emerging evidence and future perspectives. *Curr Probl Cardiol*. 2019.
- Della Corte A et al. Surgical treatment of bicuspid aortic valve disease: knowledge gaps and research perspectives. *J Thorac Cardiovasc Surg*. 2014;147:1749–1757.
- Maredia AK, Greenway SC, Verma S, Fedak PWM. Bicuspid aortic valve-associated aortopathy: update on biomarkers. *Curr Opin Cardiol*. 2017;

16. Lo YM, et al. Presence of fetal DNA in maternal plasma and serum. *Lancet*. 1997;350:485–7.
17. Lo YM, et al. Presence of donor-specific DNA in plasma of kidney and liver-transplant recipients. *Lancet*. 1998;351:1329–30.
18. Grabuschnig S et al. Putative origins of cell-free DNA in humans: a review of active and passive nucleic acid release mechanisms. *Int J Mol Sci*. 2021;21.
19. Gedvilaite V, Schveigert D, Cicenias S. Cell-free DNA in non-small cell lung cancer. *Acta Med Litu*. 2017;24:138–44.
20. Lehmann-Werman R, et al. Identification of tissue-specific cell death using methylation patterns of circulating DNA. *Proc Natl Acad Sci USA*. 2016;113:E1826–1834.
21. Pattar SK, Greenway SC. Circulating nucleic acids as biomarkers for allograft injury after solid organ transplantation: current state-of-the-art. *Transplant Res Risk Manag*. 2019;11:17–27.
22. Prasher D, Greenway SC, Singh RB. The impact of epigenetics on cardiovascular disease. *Biochem Cell Biol*. 2020;98:12–22.
23. Egger G, Liang G, Aparicio A, Jones PA. Epigenetics in human disease and prospects for epigenetic therapy. *Nature*. 2004;429:457–63.
24. Michelena HI, et al. Bicuspid aortic valve aortopathy in adults: incidence, etiology, and clinical significance. *Int J Cardiol*. 2015;201:400–7.
25. Nakamura Y, et al. The analysis of ascending aortic dilatation in patients with a bicuspid aortic valve using the ratio of the diameters of the ascending and descending aorta. *J Cardiothorac Surg*. 2014;9:108.
26. Adamo L, Braverman AC. Surgical threshold for bicuspid aortic valve aneurysm: a case for individual decision-making. *Heart*. 2015;101:1361–7.
27. Nataatmadja M et al. Abnormal extracellular matrix protein transport associated with increased apoptosis of vascular smooth muscle cells in marfan syndrome and bicuspid aortic valve thoracic aortic aneurysm. *Circulation* 2003;108 Suppl 1:1329–334
28. Liu J, Shar JA, Sucoosky P. Wall shear stress directional abnormalities in BAV aortas: toward a new hemodynamic predictor of aortopathy? *Front Physiol*. 2018;9:993.
29. Mohamed SA, et al. Inhibition of caspase-3 differentially affects vascular smooth muscle cell apoptosis in the concave versus convex aortic sites in ascending aneurysms with a bicuspid aortic valve. *Ann Anat*. 2010;192:145–50.
30. Schindelin J, et al. Fiji: an open-source platform for biological-image analysis. *Nat Methods*. 2012;9:676–82.
31. Kundaje A, et al. Integrative analysis of 111 reference human epigenomes. *Nature*. 2015;518:317–30.
32. Stunnenberg HG, International Human Epigenome C, Hirst M. The international human epigenome consortium: a blueprint for scientific collaboration and discovery. *Cell* 2016;167:1145–1149.
33. Juhling F, et al. metilene: fast and sensitive calling of differentially methylated regions from bisulfite sequencing data. *Genome Res*. 2016;26:256–62.
34. Li LC, Dahiya R. MethPrimer: designing primers for methylation PCRs. *Bioinformatics*. 2002;18:1427–31.
35. Andrews S, in <http://www.bioinformatics.babraham.ac.uk/projects/fastqc/>. (2018).
36. Sievers HH, Schmidtke C. A classification system for the bicuspid aortic valve from 304 surgical specimens. *J Thorac Cardiovasc Surg*. 2007;133:1226–33.

Publisher's Note

Springer Nature remains neutral with regard to jurisdictional claims in published maps and institutional affiliations.

Ready to submit your research? Choose BMC and benefit from:

- fast, convenient online submission
- thorough peer review by experienced researchers in your field
- rapid publication on acceptance
- support for research data, including large and complex data types
- gold Open Access which fosters wider collaboration and increased citations
- maximum visibility for your research: over 100M website views per year

At BMC, research is always in progress.

Learn more biomedcentral.com/submissions

